Assessing Lock-On Physics in Semi-Insulating GaAs and InP Photoconductive Switches Triggered by Subbandgap Excitation

Animesh R. Chowdhury, *Member, IEEE*, Richard Ness, *Senior Member, IEEE*, and Ravi P. Joshi, *Fellow, IEEE*

***Abstract*— The time-dependent photocurrent response in semi-insulating GaAs and InP was studied based on 1-D, time-dependent simulations with a focus on the Lock-On phenomenon. The results underscore the role of trap-to-band impact ionization from deep traps in rapid charge creation and its subsequent propagation much like a streamer. The numerical results compare well with the actual data. The main findings are that deeper traps nearer the valence band at higher densities, materials with larger high-field drift velocity, and cathode-side illumination would all aid in attaining Lock-On. These could be useful guidelines for producing Lock-On in new materials such as GaN for high-power applications.**

***Index Terms*— Lock-on, modeling, persistent photoconductivity, photoconductive switch, pulsed power application, semi-insulating semiconductors.**

I. Introduction

PHOTOCONDUCTIVE semiconductor switches (PCSSs) are of interest for various applications in the pulsed power arena [1]–[8], including microwave and millimeter wave generation, impulse and ultrawideband radar, particle accelerators, and directed energy systems. Potential benefits of such switches include their ultrafast turn-ON times in the picosecond regime, very low jitter response, isolation between the electrical and optical systems, and ability to scale to large voltages and currents in a single device. Semi-insulating GaAs (SI-GaAs) [9], [10] have typically been used as the PCSS elements in the past.

GaAs PCSS devices possess the capability of operating in a high gain, or "Lock-On," mode [11]. Lock-On, which occurs when the optical switch is operated above a characteristic threshold electric field, results in continued current flow even after termination of the external photoexcitation. This current endures over hundreds of nanoseconds as long as the external circuit supports the necessary electric field across the PCSS. It is an efficient mode of operation, since the optical triggering energy needed is very modest under this scenario. In the absence of Lock-On, the GaAs photoconductive switch would typically cease to conduct within a short period following termination of the optical pulse. In addition to GaAs, the Lock-On feature has been reported in other semi-insulating direct bandgap switches as well [1].

For Progress Toward Increasing the Power Levels and Switching Currents, Two Central Goals Remain: 1) attaining Lock-On in wide bandgap semiconductors such as GaN for increased voltage holdoff, power handling capability and 2) adequately understand the fundamental physics that would then allow for optimized PCSS design. The scope for optimization is broad, and encompasses choosing trap energies, their densities, the optical pulse wavelength, spatial distribution of the laser profile, and so on. In GaAs, electric fields roughly above ∼4 kV/cm were required for the onset of Lock-On, while higher fields around 14 kV/cm were reportedly needed for Fe-doped InP [12]. Lock-On has also been reported to depend on the characteristics and quality of the samples. For example, though GaAs switches containing EL2 levels exhibited Lock-On at fields in the 3.6–5.0 kV/cm range, chromium-doped GaAs samples required fields around 8.0–9.5 kV/cm [13]. The Sandia group was also able to change the GaAs Lock-On field from ∼4 to 49 kV/cm by neutron bombardment, or to 6.2 kV/cm by cooling GaAs down to 77 K [13].

Numerous theories have attempted to explain the Lock-On mechanism, including band-to-band impact ionization [14]–[16], Gunn domain formations due to satellite-valley transfers [14], [17]–[19], double injection [20], and strong carrier–carrier scattering [21]. A recent analysis [22] for SI-GaAs successfully simulated Lock-On and yielded a good agreement with the experimental data. It was shown that trap-to-band impact ionization driven by local field enhancements (associated with domain formation) plays a dominant role in helping achieve Lock-On, with photon recycling having a supportive influence. In this contribution, rough guidelines for choosing PCSS parameters that could facilitate Lock-On operation are presented, which would be useful for applications to promising new materials such as GaN.

Manuscript received April 26, 2018; revised June 17, 2018; accepted July 13, 2018. Date of publication July 31, 2018; date of current version August 21, 2018. The review of this paper was arranged by Editor J. Mateos. *(Corresponding author: Ravi P. Joshi.)*

A. R. Chowdhury and R. P. Joshi are with the Department of Electrical Engineering, Texas Tech University, Lubbock, TX 79401 USA (e-mail: chowdhuryanimesh2014@gmail.com; ravi.joshi@ttu.edu).

R. Ness is with Ness Engineering, Inc., San Diego, CA 92196 USA (e-mail: nessengr@san.rr.com).

Color versions of one or more of the figures in this paper are available online at http://ieeexplore.ieee.org.

Digital Object Identifier 10.1109/TED.2018.2856803

II. Features Relevant to Lock-On

Though triggering of the highly resistive materials into the Lock-On mode can be achieved either by laser [9]–[11] or electron-beam excitation [23], the use of subbandgap radiation is perhaps an advantageous route. This simply arises because the energy distribution of optical sources can be tailored precisely to be in accord with the desired electronic transitions; subbandgap excitation would reduce the overall energy requirement, and a more uniform generation could be achieved. An effective strategy for creating a switch with low OFF currents and high hold-off voltages would be to use shallow donors, with a larger density of deep traps to attain a fully compensated material. Focusing on a single trap level for simplicity, a trap energy E_T closer to the valence band edge E_V, would provide a larger density of electrons at the trap level. Hence, a large density of conduction electrons could be created through optical transitions from filled traps for a given laser intensity; or alternatively enable the use of lower optical intensities to create stronger levels of device current.

The physics of Lock-On can qualitatively be viewed in the following simple terms.

1) Upon photoexcitation, electron creation in the conduction band is initiated, and involves transitions from filled traps. Holes would also be formed in the valence band, and involve two separate processes:
   a) electronic transitions from the valence band into originally unfilled trap sites;
   b) transfers into trap sites that became empty following laser excitation of electrons to the conduction band from the previously occupied trap state.

   One can expect the hole density in the valence band to slightly exceed the conduction band electron density, due to the higher density of states in the valence band.
2) Considering a lateral 1-D switch geometry for simplicity, with photoexcitation focused at the center, x the densities of mobile electrons and holes would keep increasing over the pulse duration across the central portion, and spread toward the contacts at the two ends. Correspondingly, the associated conduction currents in this central region would rise, with concomitant reductions in the displacement currents associated with total current conservation. The net effect of the latter would be electric field reductions over much of the central region, while fields near the two electrodes would grow. Effectively, this would amount to the progressive "electrical shorting" at the middle section, while increasing the voltage drop across the two end zones.
3) During this time, not only are electrons and holes being added to the semiconductor system through photoexcitation but also the mobile electrons and holes acquire energy from the external field to begin participating in trap-to-band impact ionization. This ionization process is easier than the band-to-band process, because of a much lower energy threshold. The electron-initiated processes would contribute to increases in mobile electron density, while leaving behind empty traps; while hole-initiated impact ionization would result in increased hole density together with trap filling. The latter is important in replenishing the trap occupancies and making electrons available for continued trap-to-band impact ionization by the electronic process.
4) In addition, increases in hole density would effectively lead to the formation of a near space-charge neutral plasma. Near neutral space-charge neutrality ensures that electric fields and their spatial variations are maintained at a very low value within most of the photoconductive switch, while growing at the end regions. Also, the presence of such bipolar conduction can potentially lead to an S-type instability and produce downstream filamentary behavior [24]. Such filaments have been observed in photoconductive switches operating in the Lock-On mode [1], [11], [25]–[27].
5) The high fields at the end regions would easily exceed the threshold for intervalley transfer ($E_{\text{in-th}}$), if the average biasing exceeded $E_{\text{in-th}}$ value. This would help create high-field domains due to the intervalley transfer effect. High fields within domains would then function as localized sources for trap-to-band impact ionization, and fuel charge.
6) An interplay between the impact ionization (which increases local charge density) and reductions in the field due to the local space-charge enhancements would help maintain a dynamic equilibrium. The voltage drop across the circuit resistance would also contribute to limiting the total current in the PCSS. In addition, the increased fields near the cathode over time can lead to enhanced electron injection, a process expected to be stronger for anode-side illumination.

III. Model Details

A 1-D, time-dependent approach was used to solve the continuity equations based on the continuum drift-diffusion theory. The model incorporated a Poisson solver for self-consistent electric fields and contained an external circuit series resistance R_L. The inherent physical processes of the model included trap-to-band impact ionization, time- and space-dependent photoexcitation, negative differential conductance of the material, both electron and hole injection from the contacts, a trap level with associated emission and capture dynamics, and photon recycling [28]. In addition, field-driven electron emission from deep traps was included as discussed by Ganichev *et al.* [29]. Such electric-field-enhanced emission of electrons from EL3 and EL5 deep-level defects has also been reported [30]. Field-enhanced emission is expected to be important in the present context given that high fields typically arise in such applications.

Calculations of the current based on the drift-diffusion theory for a voltage supply (V_0) are given as follows:

$$\begin{aligned} dn/dt = {} & d[n(x)\upsilon_n(F) + D_n dn(x)/dx]/dx + e_{n0}(F)N_{\text{Ti}}^{-} \\ & - c_n(F)n(N_{\text{Ti}} - N_{\text{Ti}}^{-}) + nN_{\text{Ti}}^{-} \\ & \times \exp[K_{\text{electron}}(E_c - E_{\text{Ti}})/F]\beta_n\upsilon_n \\ & + K_1 \operatorname{sech}^2[(t-17)/2.5] \times \exp[\alpha|z - z_0|] \\ & + K_2 N_T^{-} \operatorname{sech}^2[(t-17)/2.5] \times \exp[\alpha|z - z_0|] \quad \text{(1a)} \end{aligned}$$

$$dp/dt = d[-p(x)v_p(F) + D_p dp(x)/dx]/dx + e_{p0}(F)(N_{Ti} - N_{Ti}^-) - c_p(F)pN_{Ti}^- + p(N_{Ti} - N_{Ti}^-) \times \exp[K_{hole}(E_{Ti} - E_v)/F]\beta_p v_p + K_1 \text{sech}^2[(t-17)/2.5] \times \exp[\alpha|z - z_0|] + K_2(N_T - N_T^-)\text{sech}^2[(t-17)/2.5] \times \exp[\alpha|z - z_0|] \quad (1b)$$

where F is the local electric field, $e_{n,p0}$ are the emission rates for electrons and holes, n and p are the electron and hole densities, $v_n(F)$ and $v_p(F)$ are the field-dependent electron and hole drift velocities, N_{Ti} and N_{Ti}^- are the total and occupied trap densities at the ith level, $K_{electron}$ and K_{hole} are the constants for ionization due to electrons and holes, while $\beta_{n,p}$ are the equivalent cross sections for the electron and hole rates. The fourth factor on the right side of (1a) and (1b) represents the rate of electron- and hole-assisted trap-to-band impact ionization. Values of the various constants given in (1a) and (1b) were given elsewhere [22]. The field-dependent drift velocities for electrons $[v_n(F)]$ and holes $[v_p(F)]$ in GaAs were taken from [31] and [32].

For InP material that is also analyzed here, the drift velocity expressions used were [33]

$$v_n(F \geq 0) = [mu_0 F + v_{sat}(F/F_{th})^4]/[1 + (F/F_{th})^4] \quad (2a)$$

for electrons with $u_0 = 0.307$ m^2/V/s, $v_{sat} = 1.25 \times 10^5$ m/s, and $F_{th} = 12$ kV/cm. The corresponding field-dependent hole drift velocity expression $[v_p(F)]$ was taken to be

$$v_p(F \geq 0) = 5.9 \times 10^3 z_h^7 - 3.1 \times 10^4 z_h^6 + 5.6 \times 10^4 z_h^5 - 3.5 \times 10^4 z_h^4 - 6 \times 10^3 z_h^3 + 1.3 \times 10^4 z_h^2 - 2.8 \times 10^3 z_h + 7 \times 10^4 \quad (2b)$$

with $z_h = (|F| - 2.3 \times 10^7)/(2.5 \times 10^7)$, and $v_p(F < 0) = -v_p(F > 0)$.

For self-consistency, the charge distributions were updated at every time step based on standard Poisson's equation. The boundary conditions for the Poisson solution were taken to be V_0 and $I(t)R_L$ at the two ends, respectively, with R_L representing the series resistance of the external circuit. The device current $I(t)$ was calculated at each time step as: $I(t) = (A/N)\sum_{j=1}^{j=N}[J_n^j(t) + J_p^j(t)] + (A\varepsilon/L)d[\Delta V(t)]/dt$, where N denotes the number of grid points along the longitudinal direction, $\Delta V(t)$ is the potential difference across the device, $J_{n,p}^j(t)$ represent the calculated electron and hole current densities, respectively, A is the device area, and L denotes the device length.

IV. Results and Discussion

1-D, time-dependent simulations for photoconductive switches (both GaAs and InP) based on the model described earlier were performed. The results obtained and implications of the parameter space on Lock-On attainability are presented and discussed in the following.

A. Role of Trap Density Initiated Ionization in Semi-Insulating GaAs Material

Simulations were first carried out for SI-GaAs. The calculated PCSS current and device voltage as a function of time in response to an external photoexcitation pulse are shown in Fig. 1. The optical pulse intensity $I(x,t)$ was taken to have the following spatiotemporal profile: $K\ \text{sech}^2[(t-17)/2.5] \times \exp[\alpha|z-z_0|]$. In the hyperbolic secant expression, t represents the time in nanoseconds, z is the position in meters, the absorption coefficient α was 300 m^{-1}, with z_0 representing the device midway point. This yielded a full-width at half maxima of ~2.2 ns, with the peak excitation set to occur at 17 ns from the start of the simulations, in keeping with the pulse parameters of Shi *et al.* [34]. A spatially symmetric profile with peak intensity located at the midway point was thus used. A single trap with energy 0.75 eV below the conduction band was assumed with a density set at 10^{22} m^{-3}. A 5-Ω series resistance was included in the circuit. The PCSS device length was taken to be 14 mm with an initial bias of 7 kV. The results of Fig. 1 show the device going into a Lock-On mode after about 20 ns, with a current that fluctuates about a mean value of 150 A. The current magnitude is comparable to values reported for SI-GaAs by various groups [11], [34]. The oscillations arise due to the evolution of the internal charge and the electric field distribution.

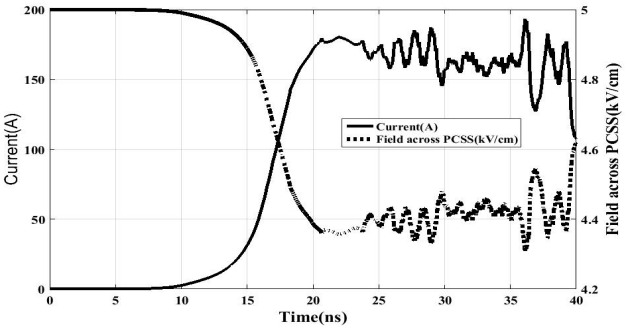

Fig. 1. Calculated PCSS current and device voltage as a function of time for SI-GaAs subjected to an external photoexcitation pulse. The trap energy was 0.75 eV below the conduction band with the trap density chosen to be 10^{22} m^{-3}.

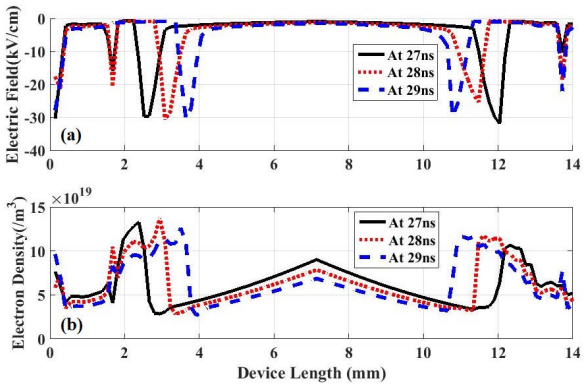

Fig. 2. Snapshots of the spatial profiles in a photoexcited GaAs PCSS at 27, 28, and 29 ns. The laser was spatially focused at the center of the device. (a) Temporal evolution of the electric field profile and (b) electron density profiles.

Fig. 2 shows the snapshots of the electric field and electron density profiles obtained at the 27-, 28-, and 29-ns time instants. The two following aspects are evident in these results: 1) the appearance of high electric field regions toward the

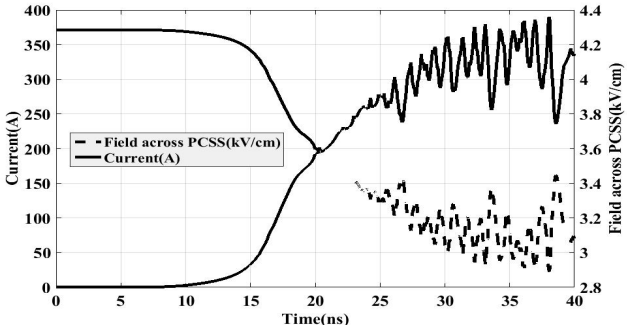

Fig. 3. Simulation results for the current and device voltage as a function of time with the same PCSS specifications as used for Fig. 1, except for a slightly higher trap density of 1.1×10^{22} m^{-3}.

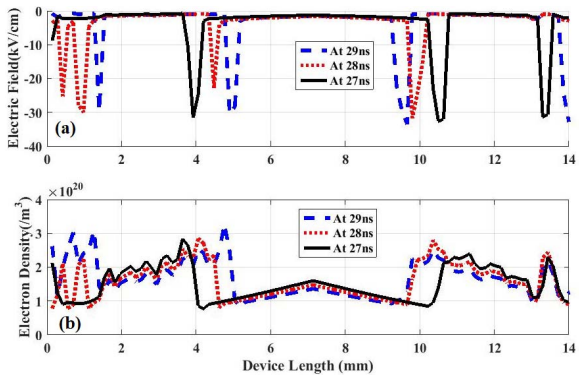

Fig. 4. Similar snapshots of the spatial profiles in the photoexcited GaAs PCSS at 27, 28, and 29 ns as in Fig. 2, but for a higher trap density of 1.1×10^{22} m^{-3}. (a) Temporal evolution of the electric field profile and (b) electron density profiles.

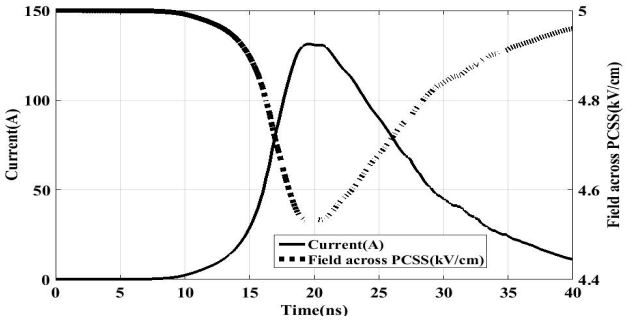

Fig. 5. Simulation result for the GaAs device current in response to the photoexcitation pulse. With trap density at 0.9×10^{22} m^{-3}, no Lock-On is predicted.

cathode (left) and anode (right) sides of the PCSS and 2) the movement of these high-field regions toward each other at large speeds of $\sim 9 \times 10^5$ m/s. These speeds are larger than the highest electron drift velocity in GaAs. This is in keeping with high velocities reported in [18] and [35]. The results suggest the following physical processes to be at work.

1) The electron density begins increasing due to the external photoexcitation.
2) The local electric fields then decrease over these regions of high carrier density, followed by a progression of the electric field to an adjacent region, much like the movement of a streamer.
3) With a shift in the electric field to an adjacent location, strong enhancements in electron density through trap-to-band impact ionization then develop.

This, in turn, lowers the local field dramatically. Thus, a positive feedback cycle with a moving charge domain is initiated.

Consider the electric field peak on the left at the 27-ns instant in Fig. 2(a). The electron density just to its left [Fig. 2(b)] is higher than the value to the right of the peak field. Consequently, over time, the peak field advances to the right (where the conduction currents were low and require a higher displacement component) from ~2.4- to 3-mm location, during the 27- to 28-ns time interval. Similarly, for the electric field peak on the right located at ~12 mm at the 27-ns instant, the movement is to the left since the electron density exhibits higher values to the right of the 12-mm location.

An important change in the photocurrent is predicted if the trap density is altered. Fig. 3 shows the simulation results for the time-dependent current and device voltages with the same PCSS specifications as used for Fig. 1, except for a somewhat higher trap density of 1.1×10^{22} m^{-3}. The current is now predicted to be much larger at around 400 A, as compared to the lower 150 A value in Fig. 1. The evolution of the field and electron density profiles is shown in Fig. 4. As compared to the previous results of Fig. 2, the electron density profile is seen to be larger by a factor of two at the higher trap density. Also, a comparison of Figs. 2(a) and 4(a) reveals that the high electric field regions tend to form sooner and start moving toward the device center. The larger speed at which charge forms would likely be due to the larger trap-to-band impact ionization at higher trap densities. Very roughly, since this ionization rate R scales as $n\ N_{\mathrm{Ti}}^{-}$, a higher N_{Ti}^{-} value (facilitated by the larger trap density) enhances the electron population (n) in the system. Since the rate R is also proportional to n, any enhancement in electron density feeds back, thereby causing larger device currents. Our simulations also showed (though not shown here) that emptying of the filled traps upon impact ionization was followed by electronic refilling from the valence band. Hole-initiated impact ionization, as well as hole emission from the empty traps, led to the attainment of a dynamic equilibrium.

Simulation runs at even higher trap densities further confirmed the above trend toward larger currents, though the results are not shown for brevity. An important inference then is that larger trap concentrations closer to the valence band work to facilitate and promote Lock-On. Conversely, a lowered presence of traps in the Si-GaAs system tended to quench Lock-On. As an example, the simulation results at a trap density of 0.9×10^{22} m^{-3} are shown in Fig. 5. The photocurrent is seen to steadily decay upon termination of the optical pulse.

B. Analyzing Effect of the Energy Level in Semi-Insulating InP Material

Having presented Lock-On simulations in SI-GaAs and the role played by the trap density in facilitating persistent

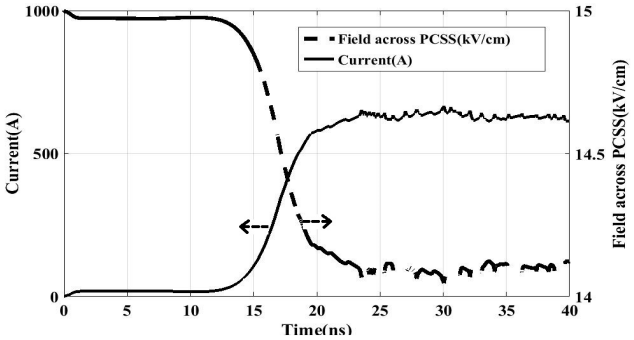

Fig. 6. Calculated photocurrent response and device voltage as a function of time for a semi-insulating InP sample subjected to an external photoexcitation pulse. A single trap level 0.34 eV below the conduction band at a density of 6.4×10^{19} m^{-3} was used.

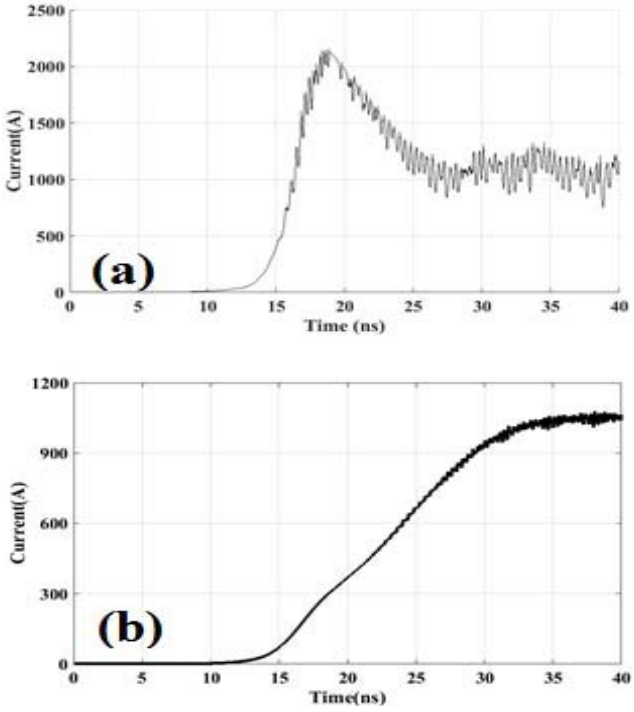

Fig. 7. Simulated PCSS current and device voltage response as a function of time in semi-insulating InP sample with trap density of 10^{22} m^{-3} and trap levels of (a) 0.75 and (b) 0.34 eV below the conduction band. The average applied bias was taken to be 8 kV/cm.

conductivity, the photo-response in semi-insulating InP was analyzed next. The primary objectives were to: 1) help provide a more complete and comprehensive analyses beyond just GaAs material; 2) have a consistency check of the physics-based model; 3) evaluate changes in the photoconductive behavior due to differences in the field-dependent velocity; and 4) assess whether the Lock-On field might be related to the intervalley transfer threshold.

Fig. 6 shows the calculated photocurrent response and device voltage as a function of time for a semi-insulating InP sample. A 21-V bias corresponding to an average field of 15 kV/cm was applied, along with a 5-Ω series resistance. The InP was taken to have a single trap level 0.34 eV below the conduction band at a density of 6.4×10^{19} m^{-3}, and conforms to values reported by Wada *et al.* [36] for InP. The velocity-field curve for InP exhibits intervalley transfer at a field of about 10 kV/cm. The main result of Fig. 6 is the existence of a persistent conductive state at an average field of 15 kV/cm. This field matches the Lock-On field for InP that has been reported in [11]. The result also shows that the intervalley transfer field (10 kV/cm) is not connected to the Lock-On field.

Next, the response in InP was compared to the predicted behavior for the SI-GaAs case. Two different simulations were carried out at an average field of 8 kV/cm, as shown in Fig. 7. The trap density was set at 10^{22} m^{-3} for both cases to match the concentration previously used for GaAs in Fig. 1. The result of Fig. 7(a) shows the InP photocurrent for a trap level at 0.75 eV below the conduction band. Though such a trap has not been reported for InP, this choice simply provides a hypothetical comparison with the GaAs material at the same defect energy. The time-dependent response of Fig. 7(a) shows Lock-On with much higher current levels than the result of Fig. 1. The increased current magnitude arises from the much larger electron drift velocity with its strong overshoot in InP, as compared to that in GaAs. For example, the drift velocity in InP at the high fields is roughly twice that of electrons in GaAs. This suggests that having a material with a larger drift velocity at high fields, rather than a high low-field mobility (as in GaAs), is an important factor from the Lock-On standpoint. Hence, attaining Lock-On in a material such as GaN, which also exhibits high electron drift velocities at large electric fields, would appear plausible. Very preliminary results from Sandia seem to show persistent photoconductivity in GaN and support the possibility of a mode similar to Lock-On [37]. The shape of the time-dependent current in Fig. 7(a) reflects the velocity overshoot characteristic. In addition, since the trap-to-band impact ionization rate is directly proportional to the drift velocity, growth in the mobile carrier density is also stronger for InP. The role played by the energy level in influencing the current magnitudes is made apparent from the results of Fig. 7(b), which were obtained at a shallower trap energy 0.34 eV below the conduction band. A simple comparison between the results of Figs. 6 and 7(b), which both had the same trap energy, reveals higher currents in the latter case, despite the lower average field used in the simulations of Fig. 7. This demonstrates that a higher trap density [6.4×10^{19} m^{-3} in Fig. 6 but 1022 m^{-3} Fig. 7(b)] can lead to much larger photoconductive currents. This occurs since traps function as a conduit for trap-to-band ionization. Furthermore, a comparison between the currents of Fig. 7(a) and (b) demonstrates that a deeper trap level is more conducive to higher current and provides easier attainment of Lock-On.

C. Probing the Role of Laser Spatial Profile on Lock-On

For completeness, the aspect of position dependent triggering of a PCSS is also discussed. Some studies seem to suggest that laser triggering at locations nearer the cathode would create higher ON-state conductances and larger currents [26], [27], [38], [39]. A more efficient use of the optical

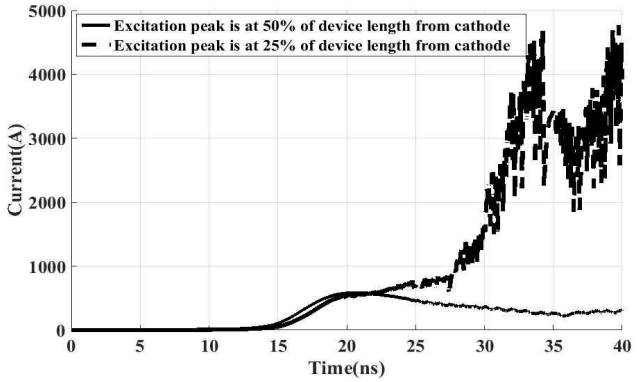

Fig. 8. Results of the time-dependent PCSS current obtained for two different locations of the laser focal point. The 25% and 50% of the device length represent the laser centered at distances of 3.5 and 7.0 mm from the left (cathode) end for the simulated 14-mm PCSS device.

trigger by focusing the beam nearer the cathode contact, and reduced switch degradation, and help to increase device longevity [26] was also demonstrated. To probe these aspects further, the present model was applied to simulate two different cases with the laser profile centered at 25% and 50% of the device length. This corresponds to distances of 3.5 and 7.0 mm from the left (cathode) end for the 14-mm PCSS device. Results shown in Fig. 8 predict higher currents with the laser nearer the cathode at 25% of the device length. This clearly shows that attaining Lock-On would then be easiest with laser illumination that was deliberately focused nearer the cathode end. Given the 1-D model, the implication is that the laser spot size should cover the PCSS width. The intensity is not as important, since as shown years ago by the Sandia group, a lower intensity (with optical energies as low as ~200–500 μJ) could still lead to Lock-On but with a longer delay time and the requirement of higher external voltages [40]. Use of optical fibers for such targeted energy delivery could be an option. With the laser centered 3.5 mm from the cathode, carrier creation predominantly occurs nearer the cathode on the left, while the high field regions are formed on the right side. Multiple field domains (not shown for brevity) were predicted to develop, and both the high electric field region and peaks in the carrier density moved toward the cathode on the left. The high field on the anode side provided greater hole injection and also enhanced hole-initiated trap-to-band impact ionization. This led the device toward a stronger two-carrier conduction scenario, and helped to increase the current density. In addition, fields were effectively reduced in the high carrier density zones and increased over the other regions; thus supporting a more effective and continued charge creation with a moving wavefront. As shown in Fig. 4, the electric fields moved in a dynamic fashion from the anode toward the cathode.

D. Qualitative Discussion

An important result that emerges from the present calculations is that the Lock-On field does not necessarily have to equal the threshold value $E_{\text{in}-\text{th}}$ for intervalley transfer. For GaAs semi-insulating devices, the observed Lock-On field values (E_{LO}) were serendipitously around the $E_{\text{in}-\text{th}}$ threshold of about 4 kV/cm. However, for InP, Lock-On has been observed to require fields on the order of 15 kV/cm, which are above the intervalley transfer threshold of 10 kV/cm for that material. In the present simulations, Lock-On was indeed predicted for InP at an average field of around 15 kV/cm in keeping with experiments. Our results suggest that Lock-On may conceivably be attainable even in wide direct bandgap materials such as GaN. Since the GaN intervalley transfer threshold ($E_{\text{in}-\text{th}}$) is high at about 150 kV/cm [41]–[43], much higher fields would be required. The more relevant factor that drives Lock-On is the local field needed for trap-to-band impact ionization. Hence, the key parameters of relevance would be the presence of a shallow donor, a relatively high density of traps close to the valence band, and a laser operating at an energy of at least ($E_C - E_T$) focused near the cathode. For example, the 532-nm laser with its photon energy of ~2.33 eV could conceivably work for GaN Lock-On.

The filamentary conduction that is often associated with Lock-On can qualitatively be understood in terms of the two-carrier conduction arising from trap-to-band impact ionization. As already obtained in this paper, this process can be driven either by electrons or holes, and would potentially give rise to an unstable S-shaped current–voltage characteristic. However, detailed analysis of this regime can only be probed through 2-D calculations, and which will be reported elsewhere. An important aspect though that could likely fuel filamentary growth is the lateral variability in work function at the metal–semiconductor contacts. The usual assumption of a uniform work function is physically incorrect. Its variation with the lateral position has been explored to some extent in the past [44]–[46]. An effective treatment of a position dependent work function variability can be based on a random variable approach, with the work function taken to have a Gaussian distribution about some mean value [47]. Nonuniformities in the work function could be further enhanced by variations in the electric field at the surface due to sharp localized geometric changes, microstructure defects, or differences in plasma densities in the semiconductor. This also then implies that since the presence of cathode-side photoexcitation will create a pool of mobile carriers at that end, the charge photogenerated would likely work to mitigate lateral inhomogeneities in the current injection. Consequently, the likelihood of filamentary growth in the PCSS can be expected to be quenched. This would provide for more stable operation, as reported in experiments [26].

V. Summarizing Conclusion

The time-dependent response of SI-GaAs and InP material to laser excitation was studied based on 1-D, time-dependent simulations. The focus was to model the Lock-On phenomenon in both semiconductor systems to demonstrate the wide applicability of the model. The additional focus was to identify parameters most relevant to bringing about Lock-On, such as the trap energy and density. It was shown that deep traps closer to the valence band, and at larger densities, foster large long-lived photocurrents. This arrangement would only require subbandgap radiation for photoexcitation, and thus provide

a more efficient switch with greater photogeneration uniformity. The simulations also underscored the role of impact ionization from trap levels. Due to this process, localized and rapid charge creations were shown to occur, pushing a local high-field region to a neighboring location, much like the dynamics of streamer propagation. Hence, fast field movements, multiple domains, and charge oscillations arose. Rapid current oscillations have been observed experimentally, and rapid propagation of density growth is also in keeping with the observed trends.

The numerical results presented here compared well with actual data obtained by Shi *et al.* [34], and those reported by the Sandia group [11]. The simulations also demonstrated that having a material with a large drift velocity at the higher fields would not only just increase the current throughput but also aid in attaining Lock-On. This was demonstrated in InP material, which has a lower low-field mobility than GaAs, but a much higher drift velocity at the higher fields. By this reasoning then, one can expect high currents and possible Lock-On in high bandgap materials such as GaN. Yet another result of this paper was the role played by the location of the illuminating optical excitation. With illumination that was deliberately centered close to the cathode contact, a much higher photocurrent was predicted, and the Lock-On seen to be easier to attain. Finally, since the presence of cathode-side photoexcitation would create a pool of mobile carriers, this charge would likely work to mitigate lateral inhomogeneities in the current injection. This would provide a more stable operation as reported in actual experiments [26]. The actual physics of filamentation, however, will require 2-D simulations, and will be reported elsewhere.

Acknowledgment

A. R. Chowdhury would like to thank the DEIS Graduate Fellowship for their support.

References

[1] A. Rosen and F. J. Zutavern, Eds., *High-Power Optically Activated Solid-State Switches*. Norwood, MA, USA: Artech House, 1993.

[2] A. Krotkus, S. Marcinkevicius, J. Jasinski, M. Kaminska, H. H. Tan, and C. Jagadish, "Picosecond carrier lifetime in GaAs implanted with high doses of As ions: An alternative material to low-temperature GaAs for optoelectronic applications," *Appl. Phys. Lett.*, vol. 66, pp. 3304–3306, Jun. 1995, doi: 10.1063/1.113738.

[3] G. J. Caporaso, Y.-J. Chen, and S. E. Sampayan, "The dielectric wall accelerator," *Rev. Accel. Sci. Technol.*, vol. 2, no. 1, pp. 253–264, 2009, doi: 10.1142/9789814299350_0012.

[4] K. S. Kelkar, N. E. Islam, C. M. Fessler, and W. C. Nunnally, "Design and characterization of silicon carbide photoconductive switches for high field applications," *J. Appl. Phys.*, vol. 100, no. 12, p. 124905, 2006, doi: 10.1063/1.2365713.

[5] S. Dogan *et al.*, "4H-SiC photoconductive switching devices for use in high-power applications," *Appl. Phys. Lett.*, vol. 82, pp. 3107–3109, Mar. 2003, doi: 10.1063/1.1571667.

[6] R. P. Joshi and D. C. Stoudt, *Photoconductive switches Wiley Encyclopedia of Electrical and Electronics Engineering*. New York, NY, USA: Wiley, 1999, doi: 10.1002/047134608X.W6025.

[7] P. Kayasit, R. P. Joshi, N. E. Islam, E. Schamiloglu, and J. Gaudet, "Transient and steady state simulations of internal temperature profiles in high-power semi-insulating GaAs photoconductive switches," *J. Appl. Phys.*, vol. 89, no. 2, pp. 1411–1417, 2001, doi: 10.1063/1.1335824.

[8] C. H. Lee, Ed., *Picosecond Optoelectronic Devices*. New York, NY, USA: Academic, 1984.

[9] D. C. Stoudt, K. H. Schoenbach, R. P. Brinkmann, V. K. Lakdawala, and G. A. Gerdin, "The recovery behavior of semi-insulating GaAs in electron-beam-controlled switches," *IEEE Trans. Electron Devices*, vol. 37, no. 12, pp. 2478–2485, Dec. 1990, doi: 10.1109/16.64521.

[10] A. S. Weling, B. B. Hu, N. M. Froberg, and D. H. Auston, "Generation of tunable narrow-band THz radiation from large aperture photoconducting antennas," *Appl. Phys. Lett.*, vol. 64, no. 2, pp. 137–139, 1994, doi: 10.1063/1.111543.

[11] F. J. Zutavern *et al.*, "Photoconductive semiconductor switch experiments for pulsed power applications," *IEEE Trans. Electron Devices*, vol. 37, no. 12, pp. 2472–2477, Dec. 1990, doi: 10.1109/16.64520.

[12] G. M. Loubriel, F. J. Zutavern, H. P. Hjalmarson, and M. W. O'Malley, "Closing photoconductive semiconductor switches," in *7th IEEE Pulsed Power Conf. Dig. Tech. Papers*, Monterey, CA, USA, Jun. 1989, pp. 365–367.

[13] G. M. Loubriel *et al.*, "Triggering GaAs lock-on switches with laser diode arrays," *IEEE Trans. Electron Devices*, vol. 38, no. 4, pp. 692–695, Apr. 1991, doi: 10.1109/16.75190.

[14] P. J. Stoudt and M. J. Kushner, "Characteristics of an optically activated pulsed power GaAs(Si:Cu) switch obtained by two-dimensional modeling," *J. Appl. Phys.*, vol. 77, pp. 3518–3522, Apr. 1995, doi: 10.1063/1.358646.

[15] H. Zhao, P. Hadizad, J. H. Hur, and M. A. Gundersen, "Avalanche injection model for the lock-on effect in III-V power photoconductive switches," *J. App. Phys.*, vol. 73, no. 4, pp. 1807–1812, Oct. 1993, doi: 10.1063/1.353190.

[16] L. Hu, J. Su, Z. Ding, Q. Hao, and X. Yuan, "Investigation on properties of ultrafast switching in a bulk gallium arsenide avalanche semiconductor switch," *J. Appl. Phys.*, vol. 115, p. 094503, Mar. 2014, doi: 10.1063/1.4866715.

[17] S. N. Vainshtein, V. S. Yuferev, and J. T. Kostamovaara, "Ultrahigh field multiple Gunn domains as the physical reason for superfast (picosecond range) switching of a bipolar GaAs transistor," *J. Appl. Phys.*, vol. 97, p. 024502, Dec. 2005, doi: 10.1063/1.1839638.

[18] L. Tian and W. Shi, "Analysis of operation mechanism of semi-insulating GaAs photoconductive semiconductor switches," *J. Appl. Phys.*, vol. 103, no. 12, p. 124512, 2008, doi: 10.1063/1.2940728.

[19] M. A. Gundersen, J. H. Hur, H. Zhao, and C. W. Myles, "Lock-on effect in pulsed-power semiconductor switches," *J. Appl. Phys.*, vol. 71, no. 6, pp. 3036–3038, 1992, doi: 10.1063/1.350988.

[20] R. P. Brinkmann, K. H. Schoenbach, D. C. Stoudt, V. K. Lakdawala, G. A. Gerdin, and M. K. Kennedy, "The lock-on effect in electron-beam-controlled gallium arsenide switches," *IEEE Trans. Electron Devices*, vol. 38, no. 4, pp. 701–705, Apr. 1991, doi: 10.1109/MODSYM.1990.200981.

[21] K. Kambour, S. Kang, C. W. Myles, and H. P. Hjalmarson, "Steady-state properties of lock-on current filaments in GaAs," *IEEE Trans. Plasma Sci.*, vol. 28, no. 5, pp. 1497–1499, Oct. 2000, doi: 10.1109/27.901221.

[22] A. R. Chowdhury, J. C. Dickens, A. A. Neuber, R. Ness, and R. P. Joshi, "Lock-on physics in semi-insulating GaAs: Combination of trap-to-band impact ionization, moving electric fields and photon recycling," *J. Appl. Phys.*, vol. 123, no. 8, p. 085703, 2018, doi: 10.1063/1.5013248.

[23] K. H. Schoenbach, V. K. Lakdawala, D. C. Stoudt, T. F. Smith, and R. P. Brinkmann, "Electron-beam-controlled high-power semiconductor switches," *IEEE Trans. Electron Devices*, vol. 36, no. 9, pp. 1793–1802, Sep. 1989, doi: 10.1109/16.34245.

[24] B. K. Ridley and T. B. Watkins, "The possibility of negative resistance effects in semiconductors," *Proc. Phys. Soc.*, vol. 78, no. 2, pp. 293–304, 1961.

[25] J. C. Adams, R. A. Falk, C. D. Capps, and S. G. Ferrier, "Dark current characterization of photoconductive switches," *Proc. SPIE*, vol. 1632, pp. 110–119, May 1992, doi: 10.1117/12.59063.

[26] G. M. Loubriel *et al.*, "Longevity of optically activated, high gain GaAs photoconductive semiconductor switches," *IEEE Trans. Plasma Sci.*, vol. 26, no. 5, pp. 1393–1402, Oct. 1998, doi: 10.1109/PPC.1997.679364.

[27] G. M. Loubriel, F. J. Zutavern, H. P. Hjalmarson, R. R. Gallegos, W. D. Helgeson, and M. W. O'Malley, "Measurement of the velocity of current filaments in optically triggered, high gain GaAs switches," *Appl. Phys. Lett.*, vol. 64, no. 24, pp. 3323–3325, 1994, doi: 10.1063/1.111266.

[28] V. Badescu and P. T. Landsberg, "Theory of some effects of photon recycling in semiconductors," *Semicond. Sci. Technol.*, vol. 8, no. 7, pp. 1267–1276, 1993.

[29] S. D. Ganichev, W. Prettl, and I. N. Yassievich, "Deep impurity-center ionization by far-infrared radiation," *Phys. Solid State*, vol. 39, no. 11, pp. 1703–1726, 1997, doi: 10.1134/1.1130157.

[30] T. Tsarova, T. Wosinski, A. Makosa, and Z. Tkaczyk, "Anisotropic electric-field-enhanced electron emission from deep-level defects in GaAs," *Semicond. Sci. Technol.*, vol. 24, no. 10, p. 105021, 2009, doi: 10.1088/0268-1242/24/10/105021.
[31] K. Yokoyama and H. Sakaki, "Importance of low-field drift velocity characteristics for HEMT modeling," *IEEE Electron Device Lett.*, vol. EDL-8, no. 2, pp. 73–75, Feb. 1987, doi: 10.1109/EDL.1987.26556.
[32] K. Brennan and K. Hess, "Theory of high-field transport of holes in GaAS and InP," *Phys. Rev. B, Condens. Matter*, vol. 29, no. 10, pp. 5581–5590, 1984, doi: 10.1063/1.336573.
[33] T. J. Maloney and J. Frey, "Transient and steady-state electron transport properties of GaAs and InP," *J. Appl. Phys.*, vol. 48, no. 2, pp. 781–787, 1977, doi: 10.1063/1.323670.
[34] W. Shi, X. Wang, and L. Hou, "Lower bound of electrical field for maintaining a GaAs photoconductive semiconductor switch in high-gain operating mode," *IEEE Trans. Electron Devices*, vol. 60, no. 4, pp. 1361–1364, Apr. 2013, doi: 10.1109/TED.2013.2244094.
[35] F. J. Zutavern, G. M. Loubriel, M. W. O'Malley, W. D. Helgeson, D. L. McLaughlin, and G. J. Denison, "Characteristics of current filamentation in high gain photoconductive semiconductor switching," in *Proc. 20th IEEE Power Modulator Symp.*, Myrtle Beach, SC, USA, Jan. 1992, p. 305.
[36] O. Wada, A. Majerfeld, and A. N. M. M. Chowdhury, "Interaction of deep-level traps with the lowest and upper conduction minima in InP," *J. Appl. Phys.*, vol. 51, no. 1, pp. 423–432, 1980, doi: 10.1063/1.327391.
[37] A. Mar *et al.*, "High-gain persistent nonlinear conductivity in high-voltage gallium nitride photoconductive switches," in *Proc. IEEE Int. Power Modulator High Voltage Conf.*, Jackson, WY, USA, Jun. 2018.
[38] B. Wang, K. Liu, and J. Qiu, "Analysis of the on-state resistance of photoconductive semiconductor switches in the non-linear mode," *IEEE Trans. Dielectr. Electr. Insul.*, vol. 20, no. 4, pp. 1287–1292, Aug. 2013.
[39] W. Shi *et al.*, "Investigation of electric field threshold of GaAs photoconductive semiconductor switch triggered by 1.6 μJ laser diode," *Appl. Phys. Lett.*, vol. 104, no. 4, p. 042108, 2014, doi: 10.1063/1.4863738.
[40] F. J. Zutavern, G. M. Loubriel, M. W. O'Malley, D. L. McLaughlin, and W. D. Helegeson, "Rise time and recovery of GaAs photoconductive semiconductor switches," *Proc. SPIE*, vol. 1378, pp. 271–280, Mar. 1991, doi: 10.1117/12.25062.
[41] R. P. Joshi, "Temperature-dependent electron mobility in GaN: Effects of space charge and interface roughness scattering," *Appl. Phys. Lett.*, vol. 64, no. 2, pp. 223–225, 1994, doi: 10.1063/1.111511.
[42] R. P. Joshi, S. Viswanadha, B. Jogai, P. Shah, and R. D. Del Rosario, "Analysis of dislocation scattering on electron mobility in GaN high electron mobility transistors," *J. Appl. Phys.*, vol. 93, no. 12, pp. 10046–10052, 2003, doi: 10.1063/1.1577406.
[43] U. V. Bhapkar and M. S. Shur, "Monte Carlo calculation of velocity-field characteristics of wurtzite GaN," *J. Appl. Phys.*, vol. 82, no. 4, pp. 1649–1655, 1997, doi: 10.1063/1.365963.
[44] R. T. Tung, "Electron transport at metal-semiconductor interfaces: General theory," *Phys. Rev. B, Condens. Matter*, vol. 43, no. 23, pp. 13509–13523, 1992, doi: 10.1103/PhysRevB.45.13509.
[45] J. H. Werner and H. H. Güttler, "Barrier inhomogeneities at Schottky contacts," *J. Appl. Phys.*, vol. 69, no. 3, pp. 1522–1533, Jan. 1991, doi: 10.1063/1.347243.
[46] L. Zheng, R. P. Joshi, and C. Fazi, "Effects of barrier height fluctuations and electron tunneling on the reverse characteristics of 6H-SiC Schottky contacts," *J. Appl. Phys.*, vol. 85, no. 7, pp. 3701–3707, 1999, doi: 10.1063/1.369735.
[47] H. Qiu, R. P. Joshi, A. Neuber, and J. Dickens, "A model study of the role of workfunction variations in cold field emission from microstructures with inclusion of field enhancements," *Semicond. Sci. Technol.*, vol. 30, no. 10, p. 105038, 2015, doi: 10.1088/0268-1242/30/10/105038.

Animesh R. Chowdhury (M'17) received the B.Sc. degree in electrical engineering from the Bangladesh University of Engineering and Technology, Dhaka, Bangladesh, in 2012. He is currently pursuing the Ph.D. degree in electrical engineering from Texas Tech University, Lubbock, TX, USA.

His current research interests include simulation and modeling in semiconductor materials, SiC and GaN photoconductive switches, and high-power semiconductor devices.

Richard Ness (M'83–SM'05) received the B.S. and M.S. degrees in electrical engineering from Texas Tech University, Lubbock, TX, USA, in 1981 and 1983, respectively.

He was with Maxwell Technologies, Inc., San Diego, CA, USA, from 1983 to 1995, where he was involved on solid-state and Thyratron modulators. He joined CYMER Inc., San Diego, CA, USA, in 1995. In 2009, he formed Ness Engineering, Inc., San Diego, CA, USA.

Ravi P. Joshi (M'83–SM'95–F'10) received the B.Tech. and M.Tech. degrees from IIT, Bombay, India, in 1983 and 1985, respectively, and the Ph.D. degree from Arizona State University, Tempe, AZ, USA, in 1988, all in electrical engineering.

He is currently a Full Professor with Texas Tech University, Lubbock, TX, USA. He has authored over 160 journal publications.